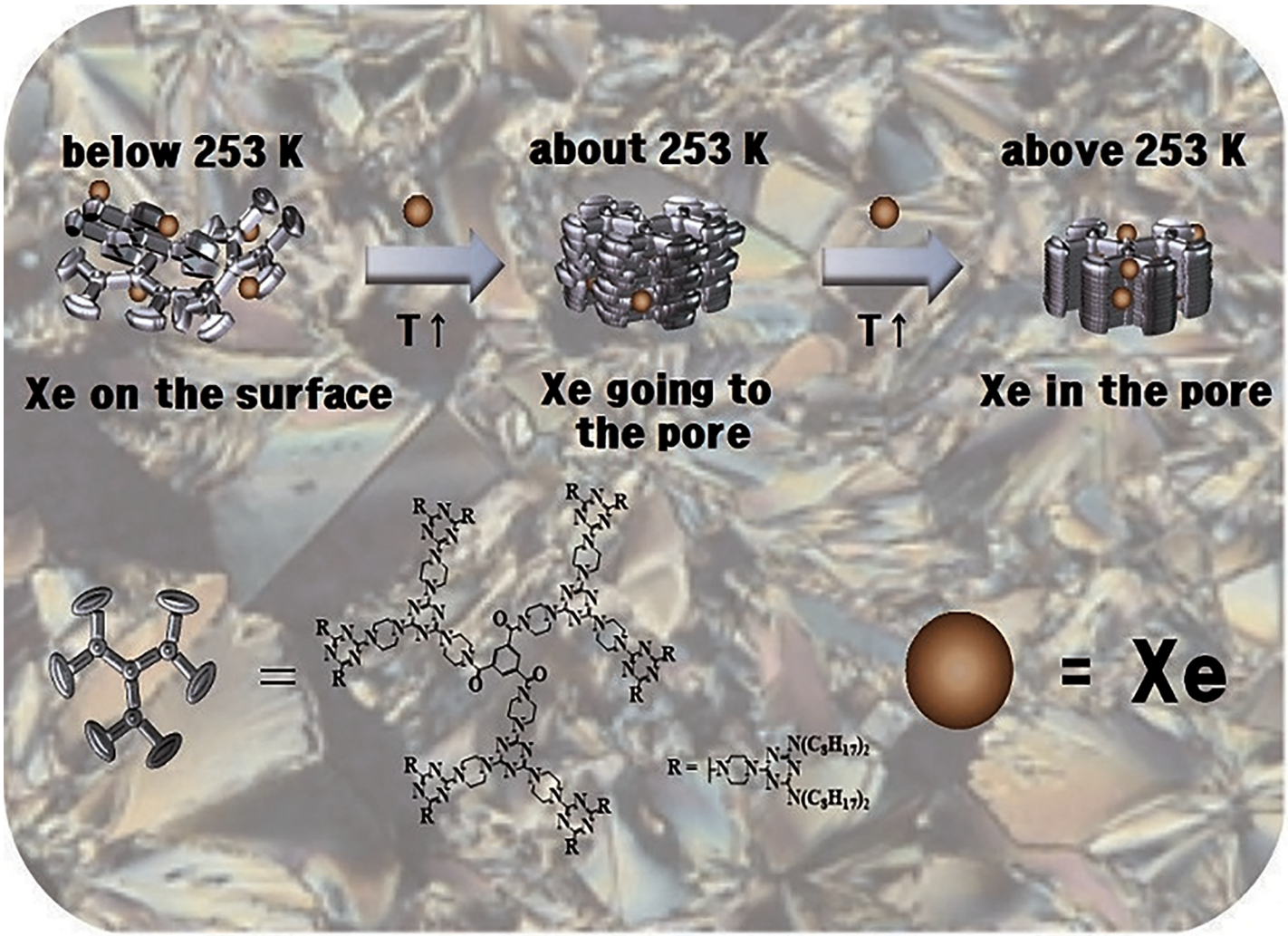

Showcasing collaborative research from National Chi Nan University and Tamkang University, Taiwan and Steacie Institute for Molecular Sciences, National Research Council, Canada.

Direct ^{129}Xe-NMR spectroscopy evidence of a mesogenic dendrimer with free void space

A dendrimer with three-fold symmetry and piperazinoamido moieties was observed to exhibit columnar phases on thermal treatment and have free void space in the mesogenic and solid states based on a ^{129}Xe-NMR study. The piperazinoamido moiety was indicated in a theoretical calculation to cause the dendritic framework to become twisted between the central core and periphery—thus resulting in the dendrimer forming a free void space inside the framework after having self-assembled into columnar stacks.

As featured in:

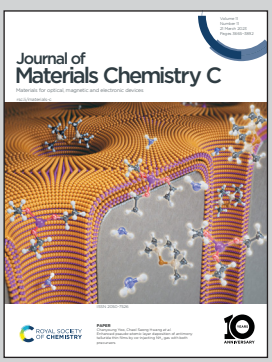

See Long-Li Lai, John Ripmeester, Hsiu-Fu Hsu *et al.*, *J. Mater. Chem. C*, 2023, **11**, 3710.

ROYAL SOCIETY OF CHEMISTRY

rsc.li/materials-c

Registered charity number: 207890

Journal of Materials Chemistry C

ROYAL SOCIETY OF CHEMISTRY

COMMUNICATION

View Article Online
View Journal | View Issue

Cite this: J. Mater. Chem. C, 2023, 11, 3710

Received 10th February 2023,
Accepted 25th February 2023

DOI: 10.1039/d3tc00486d

rsc.li/materials-c

Direct ^{129}Xe-NMR spectroscopy evidence of a mesogenic dendrimer with free void space†

Yao-Chih Lu,[a] Roberto Anedda,‡[b] Hsiu-Hui Chen,[c] Hui-Chu Hsu,[a] Shun-Ju Hsu,[a] Christopher Ratcliffe,[b] Long-Li Lai,*[a] John Ripmeester*[b] and Hsiu-Fu Hsu*[c]

A dendrimer with three-fold symmetry and piperazinoamido moieties was prepared in ~35% yield. This molecule was observed to exhibit columnar phases on thermal treatment and have free void space in the mesogenic and solid states based on a ^{129}Xe-NMR study. The piperazinoamido moiety was indicated in a theoretical calculation to cause the dendritic framework to become twisted between the central core and periphery—thus resulting in the dendrimer forming a free void space inside the framework after having self-assembled into columnar stacks.

Dendrimers, which generally consist of peripheral functionalities, linking bridges, and central cores, have definite molecular weights and predictable shapes.[1,2] They usually show three-dimensional (3-D) conformations and are likely to be soluble in most organic solvents, which is a critical advantage of dendrimers over polymers for their purification and preparation.[1,2] Since the interstitial gap between dendritic frames can efficiently adsorb metal ions or small molecules in solution, dendrimers have been broadly studied in the areas of catalysis, particle stabilization, and drug delivery.[3–14] Particularly, one or a pair of functional groups can be incorporated in the dendritic framework to impart special properties on the dendrimer.[15–21] For example, a long alkyl chain on the periphery may enable a dendrimer to exhibit liquid crystalline phases during thermal processes,[22–27] with this feature often endowing the molecule with an ability to self-assemble into a long structure and with the potential for serving as a solvating candidate for optoelectronic devices.[28–32]

On the other hand, porous materials such as metal organic frameworks (MOFs), H-bonded frameworks (HOFs), and covalent organic frameworks (COFs) are noteworthy because their void spaces inside the networks are able to accept and release guest molecules under different conditions.[33–39] Recently, like other porous materials, dendrimers as solids have also been observed to have void spaces inside the framework for guest molecules to access.[40–42] However, these solid frameworks, even when fabricated in 3-D networks, may deform or lose some of their void spaces when guest molecules are removed.[33,34,39] Therefore, it is very difficult for liquid crystalline (LC) materials, which are only constructed using 1-D or 2-D interactions, to maintain free void spaces in mesogenic or solid states. Although several reported works, such as long alkyl chains between columnar interstices of LCs or suitable dopants in mesogens with incommensurate building units, have shown the void space inside the dendrimer from indirect observations,[43–48] the evidence for the existence of free pores in LCs based on X-ray or solid-state NMR study is still unclear.[46,49] Bearing all these issues in mind, we attempted to prepare triazine-based dendrimers, having been efficiently prepared and investigated by E. Simanek, for the drug-delivering purpose.[50,51] Due to the presence of free pores in the dendrimer frameworks and due to the dendrimer arrangement being well ordered on a long range, the dendrimers should exhibit good sensitivity for detecting gases, metal ions or volatile organic compounds and have valuable applications in related areas. The three-fold symmetric dendrimer $(G_3N)_3B$ (Fig. 1) and the dendrimer $(G_3N)_2B$ were thus prepared; the molecules with three-fold symmetry were reported to self-assemble into columnar stacks and then exhibit mesogenic phases,[52,53] and indeed, $(G_3N)_3B$, as expected, was observed to exhibit a columnar phase on thermal treatment. Due to $(G_3N)_3B$ containing a non-coplanar unit, *i.e.*, the amidopiperazine moiety, on its dendritic frame, it may create a free void space in the columnar stacking, as indicated by a study involving continuous-flow variable-temperature hyperpolarized (CF-VT-HP) ^{129}Xe-NMR.[54–56] To the best of our knowledge, these

[a] Department of Applied Chemistry, National Chi Nan University, Puli, Nantou 545, Taiwan. E-mail: lilai@ncnu.edu.tw
[b] Steacie Institute for Molecular Sciences, National Research Council, Canada, 100 Sussex Drive, Ottawa, Ontario K1A 0R6, Canada. E-mail: john.ripmeester@nrc-cnrc.gc.ca
[c] Department of Chemistry, Tamkang University, Tamsui 251, Taiwan. E-mail: hhsu@mail.tku.edu.tw

† Electronic supplementary information (ESI) available. See DOI: https://doi.org/10.1039/d3tc00486d

‡ Current affiliation: Porto Conte Ricerche srl, S.P. 55 Porto Conte-Capo Caccia, Km 8.400, Loc. Tramariglio 15, Alghero (SS) 07041, Italy.

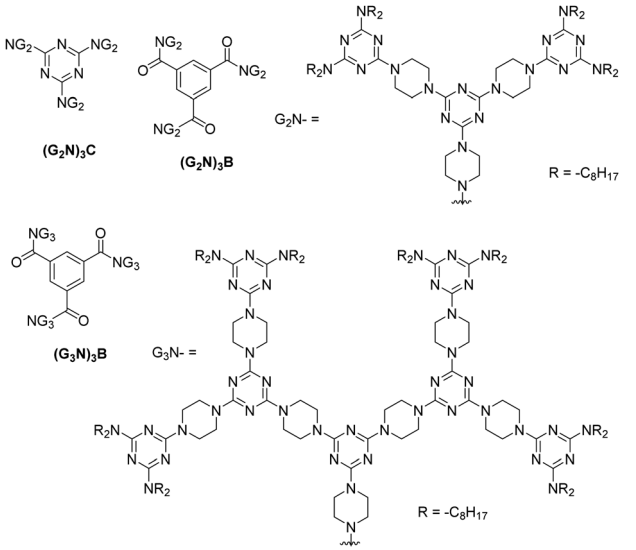

Fig. 1 Structures of **$(G_2N)_3C$**, **$(G_2N)_3B$**, and **$(G_3N)_3B$**.

preliminary results were the first direct evidence of a mesogenic dendrimer containing free void spaces in the mesogenic and solid states.

Dendrons **G_1-Cl**, **G_1-NH**, **G_2-Cl**, **G_2-NH**, **G_3-Cl**, **G_3-NH** and **$(G_2N)_3C$** were prepared according to Scheme 1, with the detailed conditions and characterizations described in the literature.[22,57] The reaction of **G_2-NH** with 1,3,5-benzenetricarboxylic acid chloride in THF, in the presence of K_2CO_3 at 170 °C for 72 hours in a sealed tube, yielded dendrimer **$(G_2N)_3B$** at ~40% yield. Similarly, the reaction of **G_3-NH** with 1,3,5-benzenetricarboxylic acid chloride gave dendrimer **$(G_3N)_3B$** at ~35% yield. The lower yield of **$(G_3N)_3B$** than that of **$(G_2N)_3B$** may have been due to the greater steric hindrance of functional groups at the periphery of dendrons of G_3-NH than that of G_2-NH.

Dendrimers **$(G_2N)_3B$** and **$(G_3N)_3B$** were characterized using ^{1}H-NMR spectroscopy and mass spectrometry. The molecular structure of **$(G_3N)_3B$** is shown in Fig. 1. Its mass spectrum, obtained using the MALDI-TOF technique, showed a peak at 9335.27, arising from the $[M]^+$ ion (Fig. S1, ESI†).

Dendrimers **$(G_3N)_3B$** and **$(G_2N)_3B$** were further characterized by performing a microanalysis, and the errors for calculated and experimental percentages for C, H and N were within 0.3%. Dendrimer **$(G_3N)_3B$** showed high thermal stability, specifically with a high decomposition temperature (T_d, 5% weight loss) of *ca.* 400 °C (Fig. S2, ESI†). **$(G_2N)_3B$** exhibited similar stability. For both dendrimers, minor weight loss was detected at *ca.* 180 °C on thermogravimetric analysis (TGA), and may have come from solvent evaporation as discussed below. The liquid crystalline properties of **$(G_3N)_3B$** and **$(G_2N)_3B$** are summarized in Table 1. For both compounds, no thermal decomposition was observed during the heating (up to 180 °C) and cooling processes. Surprisingly, **$(G_2N)_3B$** exhibited a more pronounced supercooling behaviour than did **$(G_3N)_3B$**, despite the lower molecular weight of **$(G_2N)_3B$**. Dendrimer **$(G_2N)_3B$** did not show any liquid crystalline phase on thermal treatment and only exhibited a melting point at 112 °C on heating and a solidifying point at 61 °C on cooling.

However, the dendrimer **$(G_3N)_3B$** exhibited a rectangular columnar phase during the thermal process, as evidenced by its mosaic texture under a polarizing optical microscope (POM) (Fig. 2). The corresponding range was found to be *ca.* 30 degrees in the heating process and *ca.* 89 degrees in the cooling process. The identity of the rectangular columnar phase of **$(G_3N)_3B$** was further studied using powder X-ray diffraction (Fig. 2). Two sharp peaks, at 33.88 and 28.77 Å, and indexed as *d*11 and *d*20, respectively, were observed in the small-angle region. Weak mid-angle signals were observed at 20.87, 16.96, 14.27, and 13.49 Å, which were indexed as *d*02, *d*22, *d*40, and *d*13, respectively. The lattice constants were calculated to be a = 57.54 and b = 41.92 Å. A wide-angle signal was observed at 4.66 Å, attributable to the liquid-like correlation of the molten chains. The previously reported dendrimer **$(G_2N)_3C$**,[22] also with a three-fold symmetric structure (see Fig. 1), exhibited a columnar mesogenic phase from 141 to 173 °C on heating and from 168 to

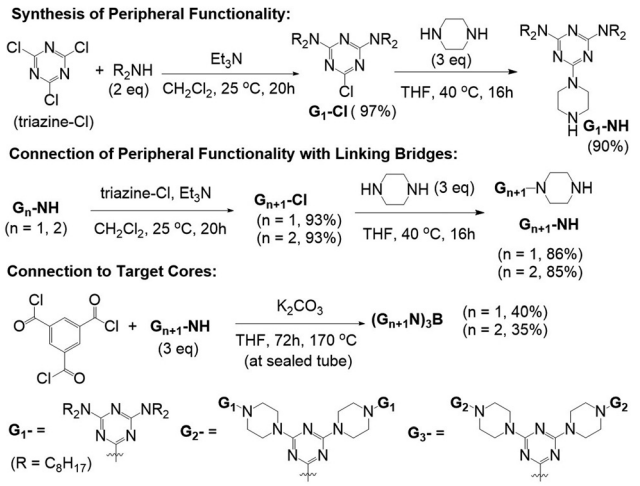

Scheme 1 Preparation of **$(G_2N)_3B$**, **$(G_3N)_3B$**, and its precursors.

Table 1 Phase transition temperatures and corresponding enthalpies (J/g), in parentheses, of dendrimers **$(G_2N)_3C$**, **$(G_2N)_3B$** and **$(G_3N)_3B$**

$(G_2N)_3C$ (MW = 4423)	Cryst	140.5 (48.3) / 135.6 (−38.2)	Col_r	172.5 (18.8) / 168.2 (−18.1)	Iso
$(G_2N)_3B$ (MW = 4504)	Cryst	111.8 (42.6) / 61.2 (−42.5)			Iso
$(G_3N)_3B$ (MW = 9335)	Cryst	142.6 (35.5) / 78.9 (−23.7)	Col_r	172.5 (2.5) / 167.7 (−2.3)	Iso

Cryst., Col_r and Iso denote the crystalline, rectangular columnar, and isotropic phases, respectively. The transition temperatures and corresponding enthalpies were recorded for the second cycles between the isotropic phases and room temperature.

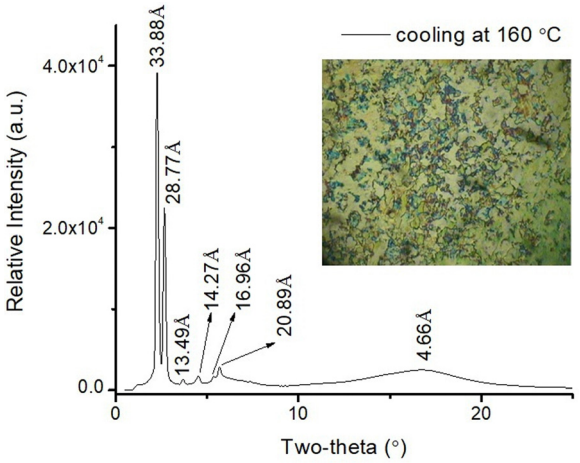

Fig. 2 POM image showing the texture and XRD pattern of $(G_3N)_3B$ at 160 °C, on cooling.

136 °C on cooling (Table 1), quite different from the thermal behaviors of $(G_2N)_3B$. Perhaps the piperazinoamido moiety in $(G_2N)_3B$ led the G_2N moiety to be non-coplanar with the benzene unit, causing difficulties for the packing of $(G_2N)_3B$ on cooling. To understand the packing differences between $(G_2N)_3C$ and $(G_2N)_3B$, the conformations of the corresponding central core moieties **1** and **2**, as shown in Fig. 3, were optimized at the Gaussian 09 at the B3LYP/6-31G** level, and the C1-N2-C3-N4(or C4) dihedral angles of **1** and **2** in the gas phase were calculated to be 5.5° and 25.0°, respectively. The calculation details are provided in ESI† (Scheme S1). The simulation results suggested all three G_2N moieties in $(G_2N)_3C$ to likely be co-planar with the triazine unit (Fig. 4), thus resulting in better stacking and favoring the formation of the columnar phase on cooling. On the other hand, the three piperazino groups being twisted by 25° relative to the central benzene ring in $(G_2N)_3B$ led the three G_2N units and 1,3,5-tricarbobenzene to be not coplanar as shown in Fig. 4, providing an explanation for the supercooling behavior observed on cooling $(G_2N)_3B$. Interestingly, including instead the larger G_3N peripheral moiety seemed to reduce the influence of the C1-N2-C3-C4 dihedral angle in dendrimer $(G_3N)_3B$, and a columnar phase was observed for $(G_3N)_3B$ on thermal treatment.

Free void spaces resulting from the twisting between the phenyl unit and piperazinoamido moiety were assumed to be maintained in the solid or mesogenic stacking of $(G_3N)_3B$. To

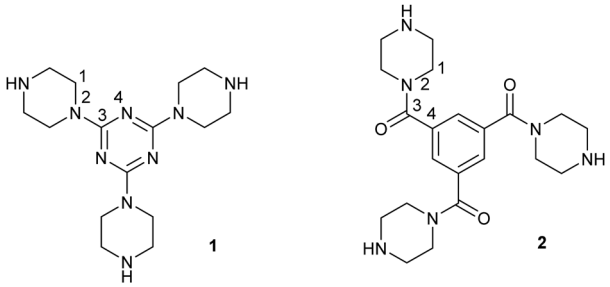

Fig. 3 Optimized conformations of **1** and **2**.

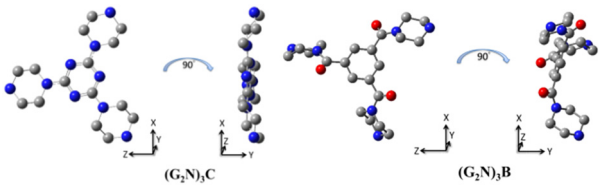

Fig. 4 Possible conformations of $(G_2N)_3C$ and $(G_2N)_3B$.

verify this assumption, dendrimer $(G_3N)_3B$ was investigated by performing CF-VT-HP ^{129}Xe-NMR spectroscopy according to the literature procedure.[54,55]

A sample of $(G_3N)_3B$ was first cooled to −100 °C (173 K) and then gradually warmed during the spectroscopic study. Up to −40 °C (233 K), only one HP-^{129}Xe signal, at 0 ppm, was observed; this signal was attributed to xenon (Xe) atoms in the gas phase. That is, below this temperature, no signal corresponding to HP Xe in the void spaces of $(G_3N)_3B$ was observed, perhaps due to either dendritic shrinkage at low temperatures hindering Xe absorption or slow diffusion of Xe within the void space causing relaxation of HP-^{129}Xe to a thermally polarized, (nearly) undetectable state. The presence of available void spaces inside the dendritic framework of $(G_3N)_3B$ was indicated by the appearance of a new peak above −40 °C (233 K), suggesting that Xe atoms were starting to freely flow through narrow void spaces within the dendrimers (Fig. 5). Chemical shifts corresponding to adsorbed Xe in the void spaces of $(G_3N)_3B$ were observed in the range 174–192 ppm. These values in general fall in the range characteristic of relatively ''tight'' void spaces, and are commonly observed for Xe dissolved in solid organic polymers or compounds with long hydrocarbon chains.[54–56] Thus, the observed signal reflected accessible pores adapted to the Xe van der Waals diameter of ~5 Å and can be taken as characteristic of Xe snugly fitting the flexible void space. The adsorption behaviour of Xe inside the $(G_3N)_3B$ framework at about room temperature (20–40 °C (293–313 K)) corresponded to the range of the solid state of the dendrimer. On further gradual warming from 293 to 313 K, a

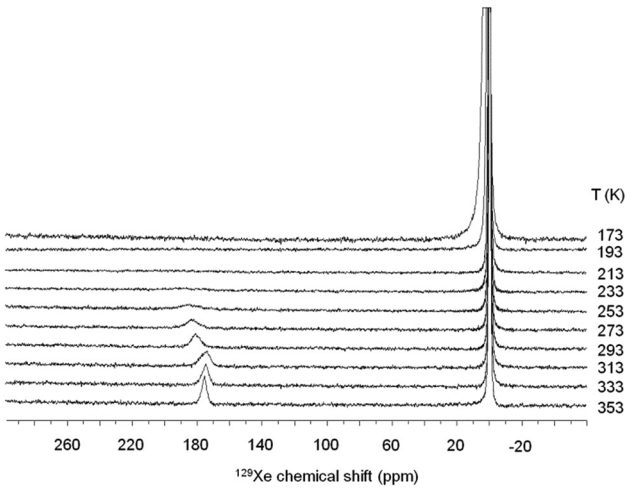

Fig. 5 ^{129}Xe-NMR spectra of $(G_3N)_3B$ on heating.

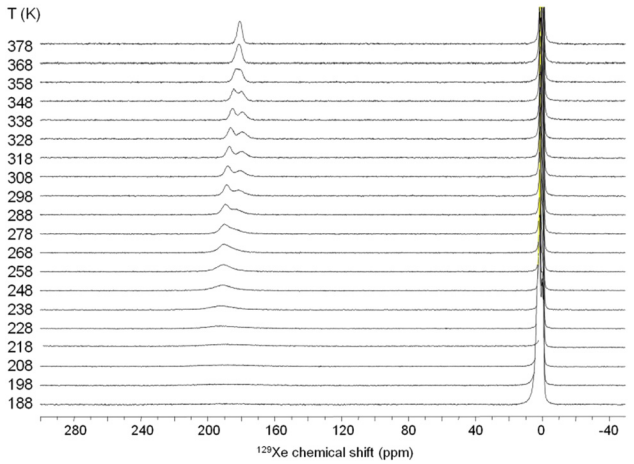

Fig. 6 ^{129}Xe-NMR spectra of **$(G_3N)_3B$** on cooling.

sudden change of the chemical shift was observed, from 183 to 175 ppm, which may have resulted from a conformational change of the dendrimer (Fig. 5). In the cooling experiment, **$(G_3N)_3B$** was first heated to the isotropic temperature and then gradually cooled during the Xe spectroscopic study (Fig. 6). The results clearly showed that in the temperature range of 85–5 °C (358–278 K), two different kinds of void spaces existed inside the **$(G_3N)_3B$** framework. Apparently, the two pores were distinct at lower temperatures but in a state of fast exchange at T > 85 °C (358 K), which in general is the temperature range at which **$(G_3N)_3B$** is in the mesogenic state. Below −5 °C (268 K), one of the signals disappeared, probably because Xe was no longer able to enter the void spaces or due to restricted diffusion of Xe within available cavities. This result further suggested the formation of different conformations of **$(G_3N)_3B$** at different temperatures as shown in the heating process; and this conformational variability may have arisen from the vibration of the piperazinoamido moiety in the **$(G_3N)_3B$** framework. Based on the results of Xe adsorption in the heating and cooling processes, it may be concluded that different void spaces formed due to the formation of different conformations of **$(G_3N)_3B$** at different temperatures. In other words, free pores were clearly indicated to exist within the **$(G_3N)_3B$** framework in both solid and mesogenic states. As indicated earlier, some weight loss was observed in the TGA study of both dendrimers, a result that can be reasonably attributed to void spaces having existed inside the dendritic framework because these void spaces would have been expected to capture solvent molecules during the recrystallization.

Conclusions

In summary, two new dendrimers with three-fold symmetry and piperazinoamido moieties were successfully prepared. The dendrimer **$(G_3N)_3B$** not only exhibited a columnar LC phase during the thermal process but also appeared to have free pores, based on the CF-VT-HP ^{129}Xe-NMR spectroscopy results. To the best of our knowledge, this was the first time that mesogenic dendrimers were observed to show such an interesting property. Dendritic columnar mesogens with rigid cores, rigid linkages, and flexible peripheral chains can be regarded as unconventional and may contain interstitial gaps between dendritic frames because their morphology is controlled by restricted conformational freedom. By properly choosing the linking functionality, free void spaces may be obtained in the corresponding mesogenic or solid states, as demonstrated here. This approach may be applied to other types of dendrimers in further research on porous mesogenic dendrimers.

Author contributions

Y. L., H. H., S. H. and L. L. were responsible for the synthesis, characterizations, and manuscript editing. H. C. and H. H. were responsible for the powder XRD experiment and the subsequent analysis. C. R., R. A. and J. R. were responsible for the ^{129}Xe-NMR experiment and the corresponding analysis. L. L., J. R., and H. H. were responsible for writing and editing the manuscript. All authors have given approval to the final version of the manuscript.

Conflicts of interest

There are no conflicts to declare.

Acknowledgements

This research was funded by the National Chi Nan University and the Ministry of Science and Technology, Taiwan (NSC 98-2119-M-260-003 and 110-2113-M-260 -001).

Notes and references

1 G. R. Newkome, C. N. Moorefield, F. Vögtle and G. Chemist, *Dendrimers and dendrons: concepts, syntheses, applications*, Wiley Online Library, 2001.
2 A.-M. Caminade, C.-O. Turrin, R. Laurent, A. Ouali and B. Delavaux-Nicot, *Dendrimers: towards catalytic, material and biomedical uses*, John Wiley & Sons, 2011.
3 K. Madaan, S. Kumar, N. Poonia, V. Lather and D. Pandita, *J. Pharm. BioAllied Sci.*, 2014, **6**, 139–150.
4 A. S. Chauhan, *Molecules*, 2018, **23**, 938.
5 Y.-H. Tang, M. Cangiotti, C.-L. Kao and M. F. Ottaviani, *J. Phys. Chem. B*, 2017, **121**, 10498–10507.
6 D. Kaur, K. Jain, N. K. Mehra, P. Kesharwani and N. K. Jain, *J. Nanopart. Res.*, 2016, **18**, 146.
7 Y. Liu, R. P. Lopes, T. Lüdtke, D. Di Silvio, S. Moya, J.-R. Hamon and D. Astruc, *Inorg. Chem. Front.*, 2021, **8**, 3301–3307.
8 K. Yamamoto, T. Imaoka, M. Tanabe and T. Kambe, *Chem. Rev.*, 2020, **120**, 1397–1437.
9 A. W. Bosman, H. M. Janssen and E. W. Meijer, *Chem. Rev.*, 1999, **99**, 1665–1688.
10 L. Röglin, E. H. M. Lempens and E. W. Meijer, *Angew. Chem., Int. Ed.*, 2011, **50**, 102–112.

11 L. Balogh and D. A. Tomalia, *J. Am. Chem. Soc.*, 1998, **120**, 7355–7356.
12 D. A. Tomalia, L. S. Nixon and D. M. Hedstrand, *Biomolecules*, 2020, **10**, 642.
13 L. Luo, J. Timoshenko, A. S. Lapp, A. I. Frenkel and R. M. Crooks, *Langmuir*, 2017, **33**, 12434–12442.
14 L. Luo, L. Zhang, Z. Duan, A. S. Lapp, G. Henkelman and R. M. Crooks, *ACS Nano*, 2016, **10**, 8760–8769.
15 R. Carloni, M. F. Ottaviani, M. Ficker and J. B. Christensen, *J. Phys. Chem. B*, 2022, **126**, 9686–9694.
16 L.-P. Wu, M. Ficker, J. B. Christensen, D. Simberg, P. N. Trohopoulos and S. M. Moghimi, *Nat. Commun.*, 2021, **12**, 4858.
17 T. Kato, J. Uchida, T. Ichikawa and T. Sakamoto, *Angew. Chem., Int. Ed.*, 2018, **57**, 4355–4371.
18 D. Yim, J. Sung, S. Kim, J. Oh, H. Yoon, Y. M. Sung, D. Kim and W.-D. Jang, *J. Am. Chem. Soc.*, 2017, **139**, 993–1002.
19 A. Nantalaksakul, D. R. Reddy, C. J. Bardeen and S. Thayumanavan, *Photosynth. Res.*, 2006, **87**, 133–150.
20 Y. Wang, X. He and Q. Lu, *Cellulose*, 2021, **28**, 4241–4251.
21 K. Albrecht, K. Matsuoka, K. Fujita and K. Yamamoto, *Mater. Chem. Front.*, 2018, **2**, 1097–1103.
22 L.-L. Lai, S.-J. Hsu, H.-C. Hsu, S.-W. Wang, K.-L. Cheng, C.-J. Chen, T.-H. Wang and H.-F. Hsu, *Chem. – Eur. J.*, 2012, **18**, 6542–6547.
23 L.-L. Lai, S.-W. Wang, K.-L. Cheng, J.-J. Lee, T.-H. Wang and H.-F. Hsu, *Chem. – Eur. J.*, 2012, **18**, 15361–15367.
24 L.-L. Lai, J.-W. Hsieh, K.-L. Cheng, S.-H. Liu, J.-J. Lee and H.-F. Hsu, *Chem. – Eur. J.*, 2014, **20**, 5160–5166.
25 M.-J. Tsai, J.-W. Hsieh, L.-L. Lai, K.-L. Cheng, S.-H. Liu, J.-J. Lee and H.-F. Hsu, *J. Org. Chem.*, 2016, **81**, 5007–5013.
26 C.-H. Lee, C.-C. Huang, C.-Y. Li, L.-L. Lai, J.-J. Lee and H.-F. Hsu, *J. Mater. Chem. C*, 2019, **7**, 14232–14238.
27 Y.-C. Lu, H.-F. Hsu and L.-L. Lai, *Nanomaterials*, 2021, **11**, 2112.
28 I. Gracia, B. Feringán, J. L. Serrano, R. Termine, A. Golemme, A. Omenat and J. Barberá, *Chem. – Eur. J.*, 2015, **21**, 1359–1369.
29 S. Mula, S. Frein, V. Russo, G. Ulrich, R. Ziessel, J. Barberá and R. Deschenaux, *Chem. Mater.*, 2015, **27**, 2332–2342.
30 P. Pieper, V. Russo, B. Heinrich, B. Donnio and R. Deschenaux, *J. Org. Chem.*, 2018, **83**, 3208–3219.
31 V. Iguarbe, J. Barberá and J. L. Serrano, *Liq. Cryst.*, 2020, **47**, 301–308.
32 A. Concellón, T. Liang, A. P. H. J. Schenning, J. L. Serrano, P. Romero and M. Marcos, *J. Mater. Chem. C*, 2018, **6**, 1000–1007.
33 Y.-F. Han, Y.-X. Yuan and H.-B. Wang, *Molecules*, 2017, **22**, 266.
34 Y.-C. Lu, C.-H. Lee, H.-H. Kuo, H.-C. Chiang, C.-T. Yao, H.-L. Sung, G.-H. Lee and L.-L. Lai, *Cryst. Growth Des.*, 2020, **20**, 6421–6429.
35 A. Moya, M. Hernando-Pérez, M. Pérez-Illana, C. San Martín, J. Gómez-Herrero, J. Alemán, R. Mas-Ballesté and P. J. de Pablo, *Nanoscale*, 2020, **12**, 1128–1137.
36 K. Geng, V. Arumugam, H. Xu, Y. Gao and D. Jiang, *Prog. Polym. Sci.*, 2020, **108**, 101288.
37 Z.-Z. Gao, Z.-K. Wang, L. Wei, G. Yin, J. Tian, C.-Z. Liu, H. Wang, D.-W. Zhang, Y.-B. Zhang, X. Li, Y. Liu and Z.-T. Li, *ACS Appl. Mater. Interfaces*, 2020, **12**, 1404–1411.
38 M. Firoozi, Z. Rafiee and K. Dashtian, *ACS Omega*, 2020, **5**, 9420–9428.
39 S. Mallakpour, E. Azadi and C. M. Hussain, *New J. Chem.*, 2021, **45**, 13247–13257.
40 Y.-C. Lu, C.-Y. Chien, H.-F. Hsu and L.-L. Lai, *Molecules*, 2021, **26**, 4862.
41 C.-H. Lee, M.-R. Tsai, Y.-T. Chang, L.-L. Lai, K.-L. Lu and K.-L. Cheng, *Chem. – Eur. J.*, 2013, **19**, 10573–10579.
42 C.-H. Lee, D. V. Soldatov, C.-H. Tzeng, L.-L. Lai and K.-L. Lu, *Sci. Rep.*, 2017, **7**, 3649.
43 K. Banlusan, E. Antillon and A. Strachan, *J. Phys. Chem. C*, 2015, **119**, 25845–25852.
44 M. Lehmann, M. Dechant, M. Lambov and T. Ghosh, *Acc. Chem. Res.*, 2019, **52**, 1653–1664.
45 M. Lehmann, M. Dechant, M. Holzapfel, A. Schmiedel and C. Lambert, *Angew. Chem., Int. Ed.*, 2019, **58**, 3610–3615.
46 M. Fritzsche, A. Bohle, D. Dudenko, U. Baumeister, D. Sebastiani, G. Richardt, H. W. Spiess, M. R. Hansen and S. Höger, *Angew. Chem., Int. Ed.*, 2011, **50**, 3030–3033.
47 M. Lehmann, P. Maier, M. Grüne and M. Hügel, *Chem. – Eur. J.*, 2017, **23**, 1060–1068.
48 M.-H. Yen, J. Chaiprapa, X. Zeng, Y. Liu, L. Cseh, G. H. Mehl and G. Ungar, *J. Am. Chem. Soc.*, 2016, **138**, 5757–5760.
49 M. Peterca, V. Percec, A. E. Dulcey, S. Nummelin, S. Korey, M. Ilies and P. A. Heiney, *J. Am. Chem. Soc.*, 2006, **128**, 6713–6720.
50 E. E. Simanek, *Molecules*, 2021, **26**, 4774.
51 S. Raut, A. E. Enciso, G. M. Pavan, C. Lee, A. Yepremyan, D. A. Tomalia, E. E. Simanek and Z. Gryczynski, *J. Phys. Chem. C*, 2017, **121**(12), 6946–6954.
52 M. Lehmann and M. Hügel, *Angew. Chem., Int. Ed.*, 2015, **54**, 4110–4114.
53 M. Peterca, M. R. Imam, C.-H. Ahn, V. S. K. Balagurusamy, D. A. Wilson, B. M. Rosen and V. Percec, *J. Am. Chem. Soc.*, 2011, **133**, 2311–2328.
54 A. V. Nossov, D. V. Soldatov and J. A. Ripmeester, *J. Am. Chem. Soc.*, 2001, **123**, 3563–3568.
55 R. Anedda, D. V. Soldatov, I. L. Moudrakovski, M. Casu and J. A. Ripmeester, *Chem. Mater.*, 2008, **20**, 2908–2920.
56 D. Wisser and M. Hartmann, *Adv. Mater. Interfaces*, 2021, **8**, 2001266.
57 L.-L. Lai, L.-Y. Wang, C.-H. Lee, Y.-C. Lin and K.-L. Cheng, *Org. Lett.*, 2006, **8**, 1541–1544.

